32

Measurement of Liquid Velocity and Liquid Distribution in a Packed Bed Using Electrical Resistance Tomography

H. D. Doan and A. Lohi
Department of Chemical Engineering, Ryerson University, Toronto, ON, Canada

1. Introduction

Packed beds are widely used in industrial mass transfer operations, including absorption, stripping, adsorption and distillation. The packing material offers a large surface area available for heat and mass transfer between gas-liquid or fluid-solid phases for a given volume. Distillation, absorption, adsorption and extraction are typical applications of packed columns. In the design of a packed column, the averaged mass transfer coefficient is usually used and assumed to be constant at all locations in the column. This is due to the fact that studies of mass transfer in a packed bed are generally based on a macroscopic approach. In this approach, the averaged mass transfer coefficient is determined based on the conditions of the inlet and outlet streams without consideration of local fluid dynamic and local mass transfer at different locations within the bed. Local mass transfer in a packed bed is in fact dependent on local liquid velocity. The local mass transfer coefficient thus varies with locations in the packed bed due to the variation of velocity and the random nature of liquid spreading in the bed. Therefore, the use of the averaged mass transfer coefficient often renders uncertainty in design and scaling-up of a packed column.

Among different methods, dissolution (Kumar et al., 1977; Sedahmed et al., 1996; Guo and Thompson, 2001) and gas absorption (Aroonwilas et al., 2003; Linek et al., 2001) are the two popular methods that have been used to obtained the average mass transfer coefficient. More recently, direct measurements of the local mass transfer coefficient in a packed bed was developed using an electrochemical technique (Gostick et al., 2002), and a mathematical model for local mass transfer coefficient in a packed bed was proposed (Dang-Vu et al., 2006a). The mass transfer coefficient is strongly dependent on liquid distribution in a packed bed. Liquid distribution is in turn dependent on the packing size and type, and the design of the liquid distributor.

Several studies on liquid velocity and distribution in a packed column have been carried out using different techniques, such as: liquid collecting method (Hoek et al., 1986; Kouri and Sohlo, 1996; Dang-Vu et al., 2006b), tracing method (Macias-Salinas and Fair, 1999; Inglezakis et al., 2001), conductance probe (Tsochatzidis et al., 2002), and tomographic measurements (Loser et al., 1999; Reinecke and Mewes, 1997; Yin et al., 2002; Bolton et al., 2004; Ruzinsky and Bennington, 2007). The liquid collecting method has been used widely to investigate liquid distribution in a packed column due to its simplicity in measurements

(Hoek et al., 1986; Kouri and Sohlo, 1996; Farid and Gunn, 1978; Kunjummen et al., 2000). In this method, liquid is collected in an array of cells or concentric cylinders at the bed outlet. The liquid collecting duration is also recorded. Liquid velocity obtained from the measured liquid volume is then used to quantify the liquid distribution in the bed. However, the liquid velocity obtained from the liquid collecting method is an axially aggregated flow through the packed bed at a certain radial location, which doesn't reveal the local liquid distribution at various axial distances along the bed. Therefore, in the present study measurements of liquid distribution and velocity at various axial distances in a packed bed were carried out, using electrical resistance tomography (ERT). The ERT system can quantify the liquid distribution and liquid velocity in the packed bed without disturbing the flow field since it is a non-intrusive technique. In addition, measurements at different locations in the packed bed can be measured simultaneously without the need for changing the bed height, which is of advantage over the liquid collecting method.

2. Experimental method

2.1 Apparatus for the electrical resistance tomography

The experimental apparatus consists of a 0.3-m diameter column filled with 2.0-cm polypropylene spheres as shown in Figure 1. The packed bed height of 6 times the column diameter was used. An ERT system (model P2000, Industrial Tomography Systems Ltd., Manchester, UK) was used to measure the flow pattern at 6 axial positions in the packed bed using 6 electrode planes (P1 to P6) located at equal-distance of 0.30 m apart along the axial direction of the bed. In order to avoid disturbance to the flow, electrodes were installed flush with the inside wall of the column. At each electrode plane, 16 stainless-steel electrodes (1.0 cm x 2.0 cm) were arranged at equal distance one to another on the perimeter of the column (Figure 2). All electrodes on the 6 planes were connected to a data acquisition system for data collection. Experiments were performed with a high conductivity tracer (a sodium chloride solution) introduced into the liquid inlet to create a high conductivity front that moved through the packed bed.

In the present study, an electric current was applied to two neighbouring electrodes (e.g. electrodes 1 and 2), and then voltages were measured from the remaining pairs of neighbouring electrodes (e.g. 3 and 4; 5 and 6 .etc...). The electric current was then applied through the next pair of electrodes and the voltage measurements were repeated. Measurements were made within each plane separately and concurrently. 104 individual voltage measurements were collected from each of the 6 planes of electrodes every 100 ms (sampling interval). Those 104 measurements constitute a measurement set. The number of samples per frame (the number of measurement sets that were taken to produce an average frame of data) was set at 8. From the voltage measurements, the ITS System 2000 software uses a linear back-projection image-reconstruction algorithm to convert the data to tomograms that showed the distribution of liquid flow on a 2D plane.

Both upward and downward flow modes were used in the experiments. For the upward flow mode, water was pumped continuously from a holding tank to the bottom of the column. The liquid flow rate was monitored by a rotameter (Model F-45750-LHN12, Fabco Co., Maple, Ontario, Canada). A 0.5% wt salt solution (conductivity = 9.95 $mS.cm^{-1}$) was used as the high conductivity tracer. Five liquid flow rates from 8.83 – 12.6×10^{-4} $m^3.s^{-1}$ (14–20 gpm) were used in the experiments. When the water flow rate in the column had reached a steady state, a 1L aliquot of the tracer solution was injected into the liquid inlet stream to the

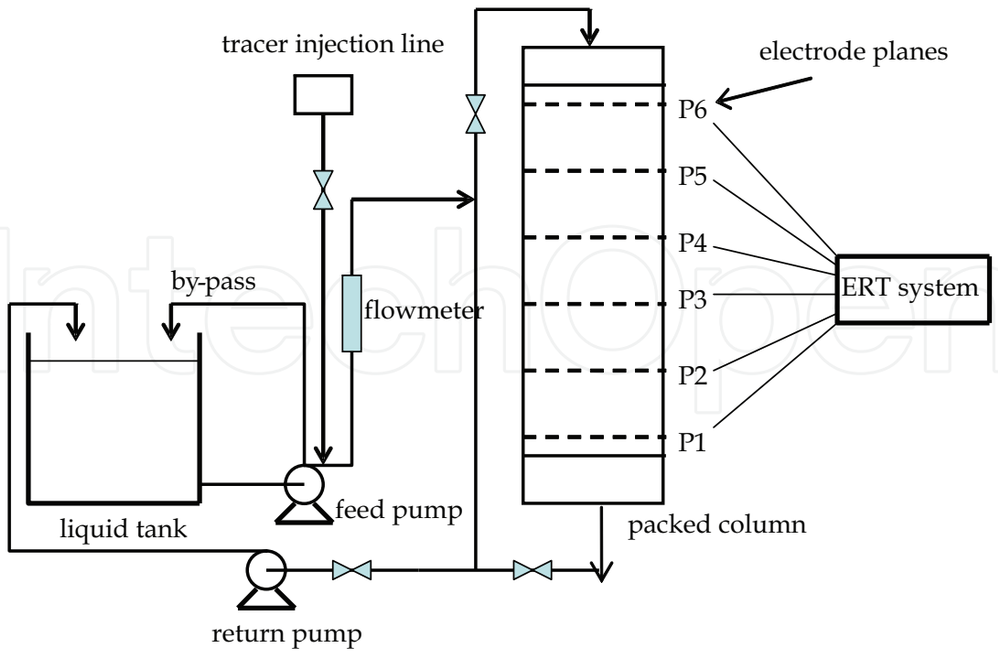

Fig. 1. Schematic diagram of the experimental set-up for ERT

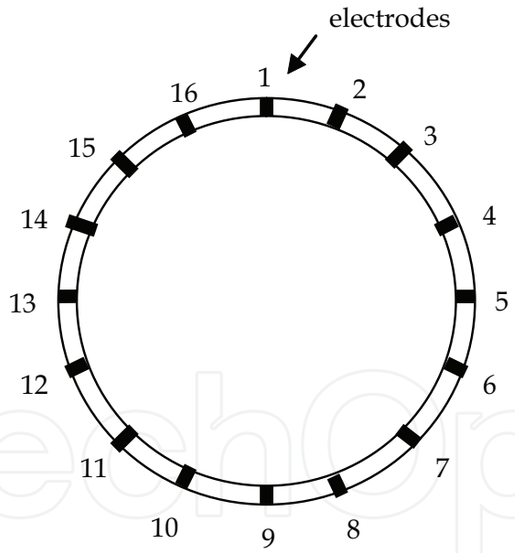

Fig. 2. Arrangement of the electrodes on the column wall

column. A reference in the ERT system was taken before the injection of the tracer. This reference acted as a base line from which the increase in the conductivity was observed when the tracer reached the electrodes. This reference conductivity was about 1.00 $mS.cm^{-1}$. The ERT system recorded the conductivity profiles at 6 planes along the column simultaneously.

For the downward flow mode, water was pumped to the top of the column. A 1.5% wt salt solution (conductivity = 29.9 $mS.cm^{-1}$) was used as the tracer for better conductivity measurements due to the liquid hold up and channelling that tended to dilute the tracer

more. Similar conductivity measurement procedure to that for the upward flow was used at various flow rates from 5.05 – 7.57×10^{-4} m^3.s^{-1} (8–12 gpm).
Following the acquisition of data from the boundary of the object to be imaged it is necessary to process this data using an appropriate image reconstruction algorithm. For an ERT system the reconstructed image will contain information on the cross-sectional distribution of the electrical conductivity of the contents within the measurement plane. A square grid with 20 x 20 = 400 pixels represents the vessel interior cross-section. Some of these pixels will lie outside the vessel circumference and the image is therefore formed from the pixels inside the vessel. The circular image is constructed using 316 pixels from the 400 pixel square grid as shown in Figure 3 (ITS System 2000 Version 6 User's Manual, Industrial Tomography System Ltd., Manchester, UK).
The conductivity values of individual pixels can be exported to an Excel file for further analysis. From the time elapse between the advancement of the conductivity peak of an individual pixel from one plane to the next one, the local liquid velocity was determined. From the values of the local velocities, the liquid distribution factor was calculated using Equation (1) below. These values were then compared with the values obtained from the liquid collecting method that is described in the following section.

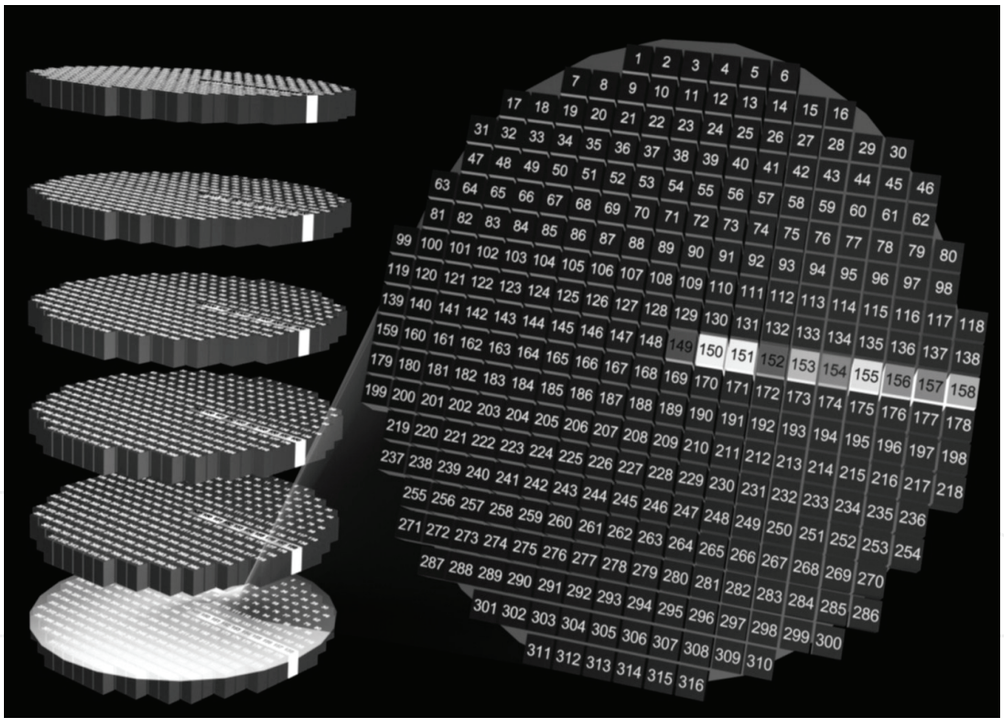

Fig. 3. ERT grid of 316 pixels for the image reconstruction

2.2 Apparatus for the liquid collecting method

In the investigation of liquid distribution, the same 0.3 m diameter PVC column filled with 2.0-cm polypropylene spheres as shown in Figure 1 was used. However, a liquid collector was added to the column as shown in Figure 4. For liquid distribution measurements using the liquid collecting method, only water was used. Two liquid flow rates of 5.05×10^{-4} m^3.s^{-1} and 7.57×10^{-4} m^3.s^{-1} (8 gpm and 12 gpm) were used. For a comparison with the ERT method,

in which only liquid was used, the gas blower was turned off in these experiments. Liquid flowing down the bed was collected in a collector with 39 tubes of 25.4-mm diameter. The tubes were arranged circularly at four different radial positions as shown in Figure 5.

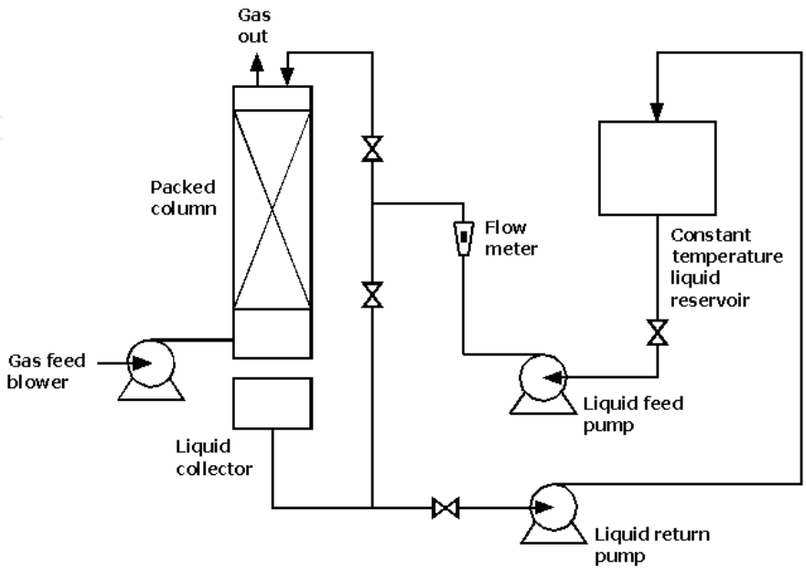

Fig. 4. Experimental set-up for the liquid collecting method

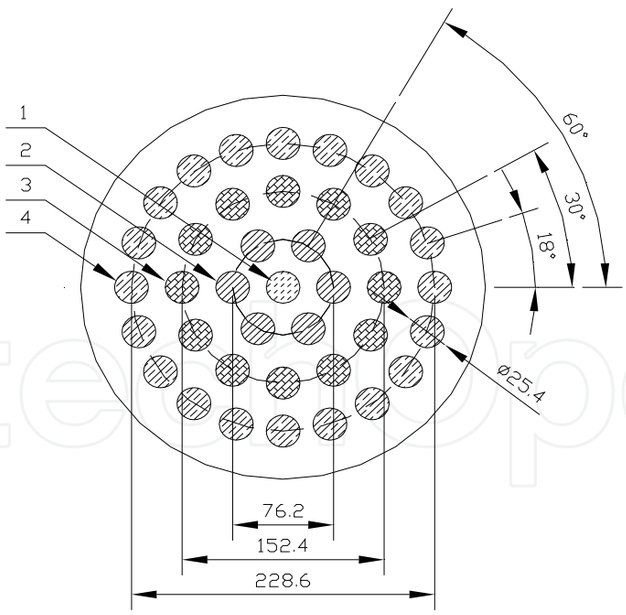

Fig. 5. Schematic diagram of the arrangement of in the liquid collecting tubes: 1. Center section with 1 tube; 2. Inner section I with 6 tubes; 3. Inner section II with 12 tubes; and 4.Outer section with 20 tubes (dimension unit: mm)

Measurements were carried out at three axial levels from the top of the packing: 0.3, 0.6 and 0.9 m. These are equivalent to the ratios of the packing height to the column diameter, x/D,

of 1, 2 and 3. The wall flow was separated from the bulk flow in the packing by an annular ring on the inside wall of the column at the packing support level and collected in a separate container so that it did not interference with the local liquid flow through the packing to the liquid collector described above.

In order to quantify liquid distribution in the packed bed, a liquid distribution factor was used and defined as below (Dang-Vu et al., 2006b):

$$M_F = \frac{1}{n}\sqrt{\sum_{i=1}^{n}\left(1-\frac{V_i}{V_{AVG}}\right)^2} \quad (1)$$

where M_F is the liquid distribution factor, n is the number of liquid collecting tubes, V_i is the liquid velocity to individual collecting tubes and V_{AVG} is the averaged liquid velocity

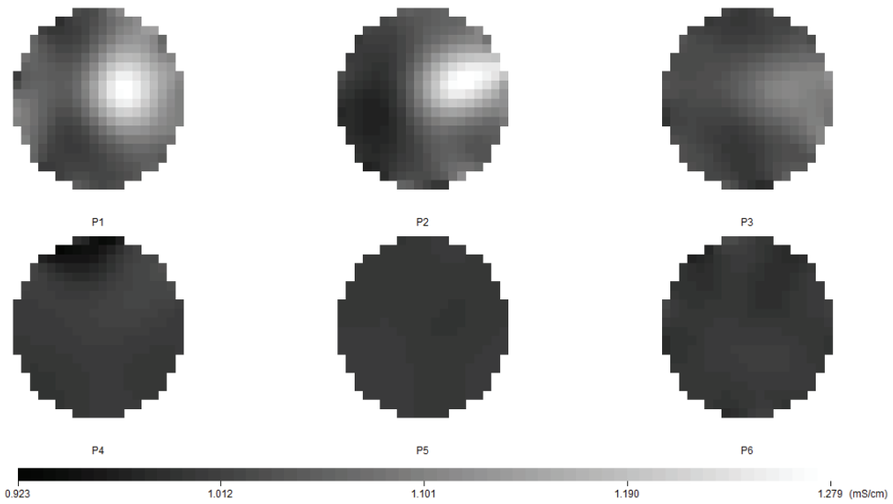

6(a)

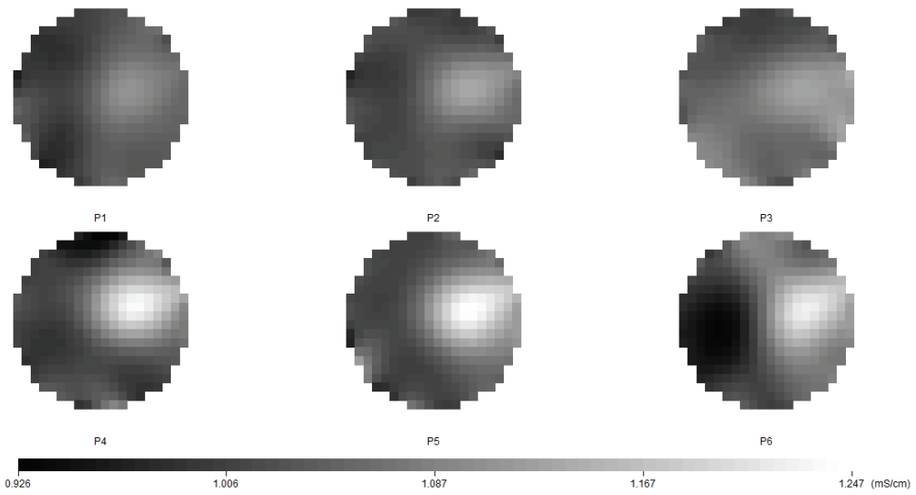

6(b)

Fig. 6. Tomographic images of the conductivity at various planes for upward flow

3. Results and discussion

3.1 Upward flow profile

For the upward flow mode, the high conductivity tracer moved upward with the bulk flow and passed plane 1 to plane 6, consecutively, after the tracer injection. The advancement of the tracer upward through the column can be seen in the tomograms in Figures 6(a) and 6(b). The shade of a region in a tomogram indicates the conductivity of that region in accordance with the conductivity scale in mS/cm as shown below the tomograms.

Some time after the tracer injection, the high conductivity solution reached planes 1 and 2 as indicated by the light spots in the tomograms for P1 and P2 in Figure 6(a). The tomograms at planes 3 to 6 still have a dark shade indicating a low conductivity of the bulk water stream since the tracer solution didn't reach to those planes yet. As time went by, the tracer solution moved farther upward to P4, P5 and P6 as can be seen by the high conductivity regions (light shade) in Figure 6(b) while the conductivities at P1, P2 and P3 decreased (dark shade at those planes) since the tracer solution had moved out of those regions.

Using the mean conductivity data across a plane, conductivity peaks can be identified when the tracer has reached successive planes as shown in Figure 7. The distance between the peaks represent the time for the tracer to move between the planes. From the conductivity peaks and the time elapsed between two peaks, the liquid velocity from one plane to the next one was determined. It was noted that in the upward flow mode, a steady flow and a more even distribution of conductivity across a plane were obtained. The velocities at different planes are comparable to one another and the average velocity throughout the packed bed. This might be due to the fact that the liquid almost moved up the column in a plug flow pattern. The flow pattern wasn't distorted by liquid hold-up or liquid channelling. The ERT measurements of the liquid velocity were within 5% with the interstitial velocities calculated from the averaged liquid flowrate measured by a flowmeter and the bed porosity (Figure 8).

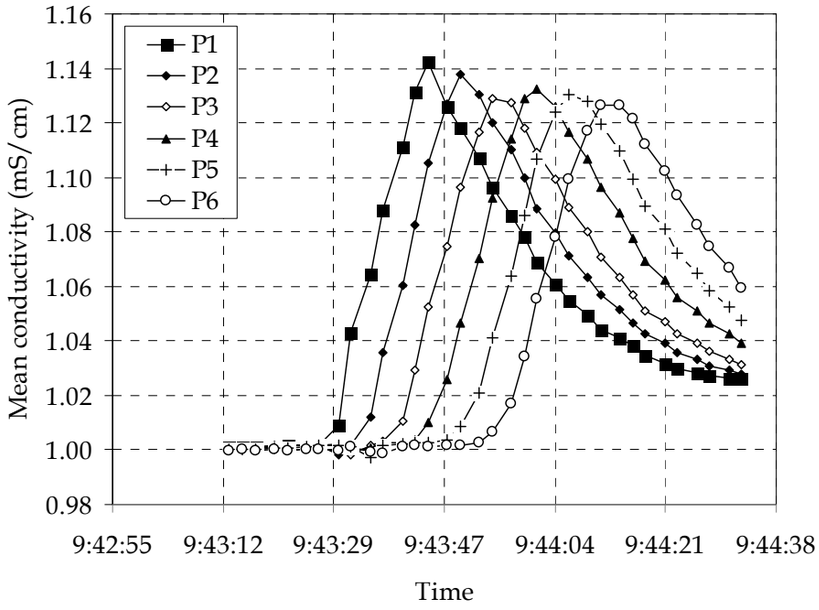

Fig. 7. Mean conductivity at various planes for the upward flow

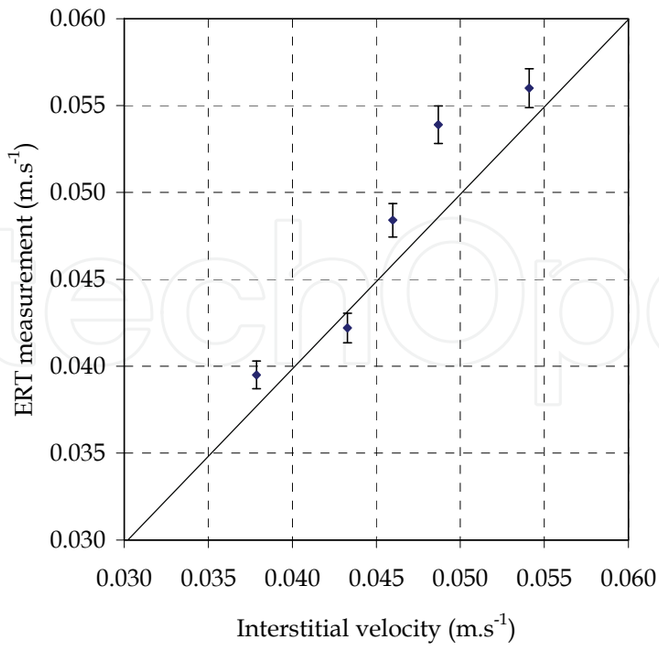

Fig. 8. Comparison of liquid velocity measured by the ERT and the flowmeter

3.2 Trickle flow profile

Tomograms for the trickle flow mode are shown in Figures 9(a) and 9(b). In addition, the variations of the mean conductivities at individual planes with time are presented in two separate graphs, for clarity, in Figures 10(a) and (b). Tomographic images were recorded at six different heights downstream from the top of the column. The high conductivity tracer moved from plane 6 (P6) downwards to plane 1 (P1) after injection, as indicated by the high conductivity regions of light shade in the tomograms in Figures 9(a) and 9(b). When the column is operated in the trickle flow mode, the advancement of the high conductivity plane was not as clear as those obtained with the upward flow. The tomograms show successive increases in conductivity from plane 6 (P6) at the top of the bed to plane 1 (P1) at the bottom of the bed. However, the high conductivity liquid remains at a plane for a period longer than that observed with the upward flow mode. At times, high conductivity profiles of multiple planes overlapped since the high conductivity front didn't move from one plane to another in pulses, i.e. no distinctive peaks at individual planes at different time steps. Less pronounced and broader mean conductivity distribution was observed as shown in Figures 10(a) and (b). This might be due to liquid hold-up in the packed bed under the trickle flow mode. Liquid tends to linger in the void space of the packing before moving downward the column.

For the trickle flow, the conductivity peaks were not very distinctive from one plane to another. Therefore, liquid residence time in the column was used as an indicator for the liquid flow. A theoretical residence time was also calculated using the interstitial liquid velocity, which was determined from the average flow rate measured by a flowmeter and the void fraction of the bed. The ERT-measured residence time was shorter at a higher flow rate, as expected. The residence time determined from the ERT data also followed a trend similar to that of the theoretical residence time, as shown in Figure 11. For varied liquid flowrates from 5.05 – 7.57×10^{-4} $m^3.s^{-1}$, the theoretical residence times were about 1.5 -2.0

times those predicted from the ERT data. It appeared that the deviation between the two residence times increased with liquid flow rate. The theoretical residence time based on the volumetric flow rate measurement and the bed void volume was unable to account for the effect of the liquid hold–up, the liquid channelling and the wall flow in the packed bed. In addition, it is relevant to note that the theoretical residence time was based on the whole void space, and the liquid was assumed to fill all the void space in the packed bed before eluting out at the bottom of the column. As a result, the residence time tended to be long. On the other hand, the actual liquid flow might have channelled through the packed bed; hence, by-passed some of the void space resulting in a shorter residence time as shown by the ERT measurement. This might be considered as an advantage of the ERT system in capturing the real flow distribution in the packed bed.

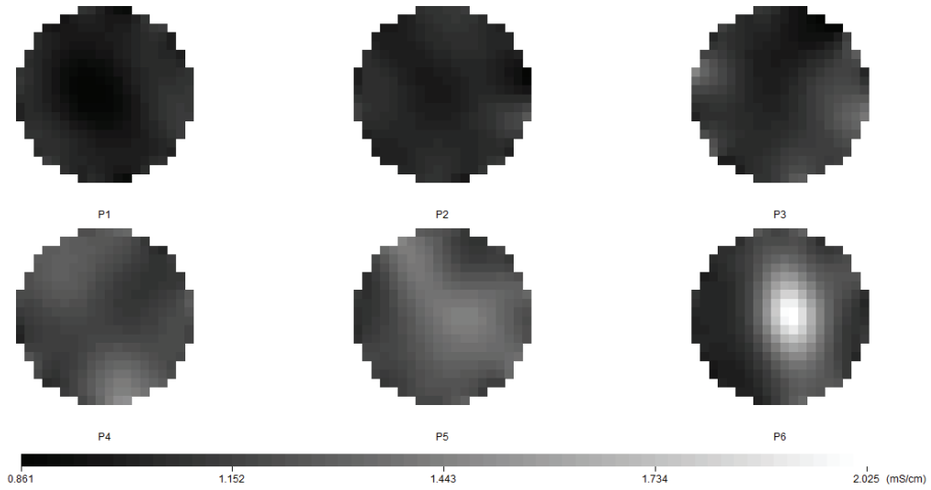

9(a)

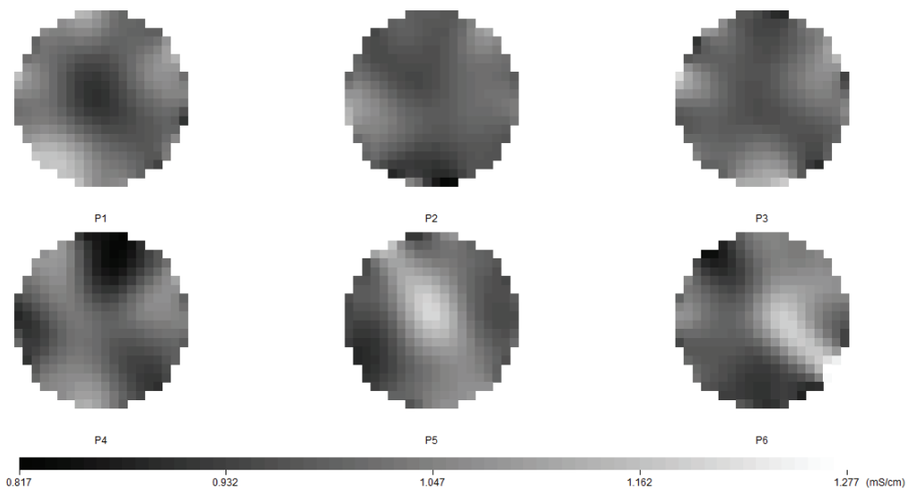

9(b)

Fig. 9. Tomographic images of the conductivity at various planes for trickle flow

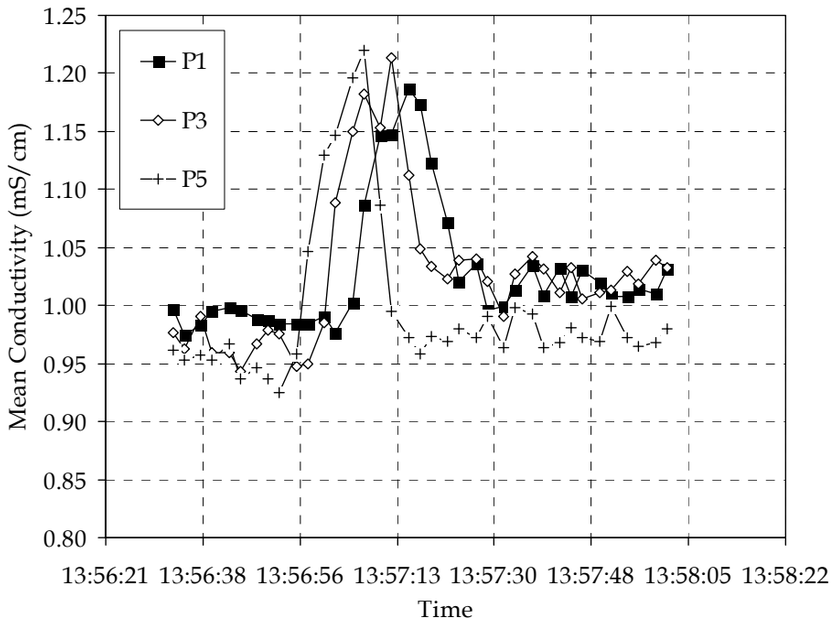

10(a)

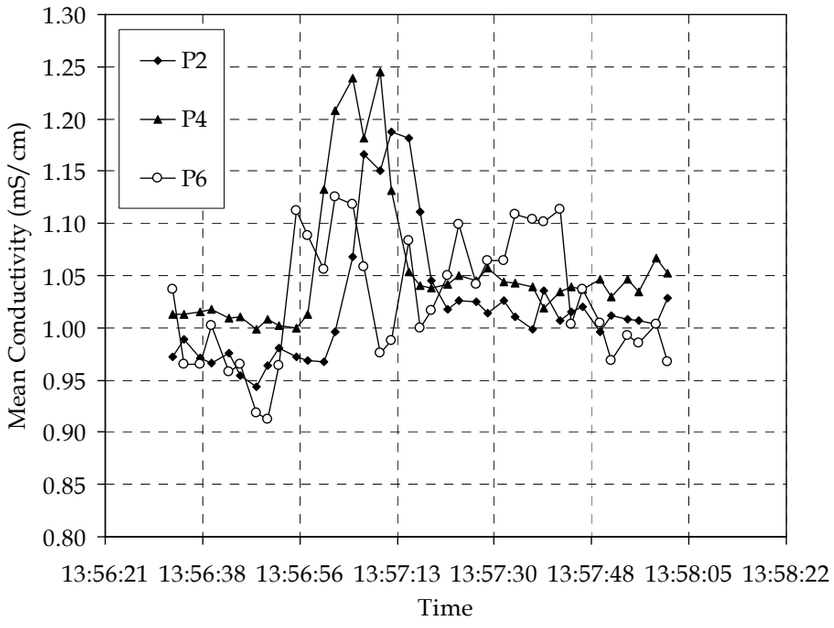

10(b)

Fig. 10. Mean conductivity at various planes for the trickle flow

Liquid distribution factors estimated by Equation (1) using the liquid velocities obtained by the liquid collecting method and the ERT method at two liquid flowrates are plotted in Figure 12. As can be seen in Figure 12, the liquid distribution factor obtained from the ERT technique follows a similar trend of that obtained from the liquid collecting method. This indicates that the ERT method was suitable for the measurement of liquid distribution in a packed column. Moreover, the ERT method allows for measurements of liquid distribution at multiple axial

distances concurrently. This is an advantage over the liquid collecting method, which can only measure the aggregated liquid distribution at one bed height at a time.

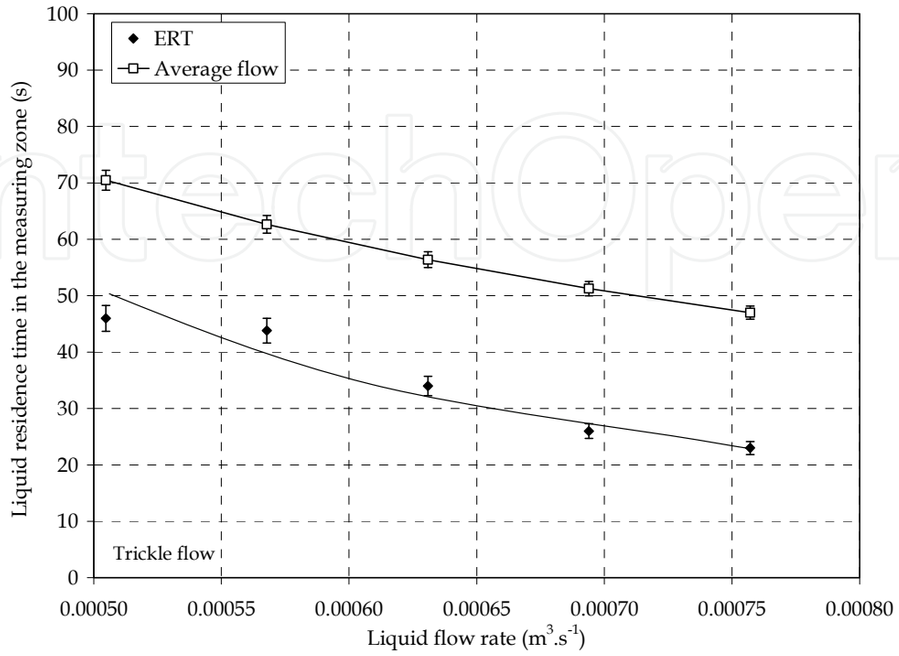

Fig. 11. Liquid residence times estimated from the ERT measurements and the calculated values from the average flowrate measured by a flowmeter

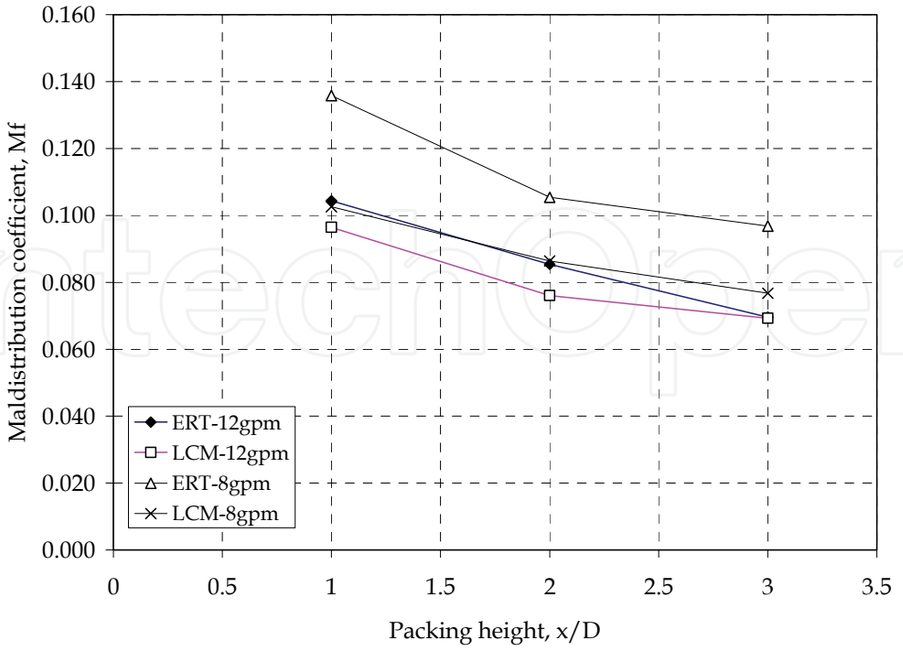

Fig. 12. Liquid distribution factor obtained by the liquid collecting method and the ERT technique

As can be seen in Figure 12, the liquid distribution factor decreased with the bed height and liquid flowrate, as expected. This is in agreement with the results obtained and reported by other researchers (Hoek et al., 1986; Kouri and Sohlo, 1996; Dang-Vu et al., 2006b). At both liquid flowrates, the liquid distribution factors obtained by the ERT method are higher than those obtained by the liquid collecting method. This might be due to the fact that the number pixels used in the ERT method was 316, i.e. the cross-sectional area of the column was divided into 316 segments, while the number of liquid collecting tubes was only 39. The liquid streams collected in the collecting tubes covered a significant portion of the cross-sectional area of the column as compared with the local velocities obtained by the ERT method. Therefore, the liquid streams collected in the liquid collecting method were averaged out resulting in a more even liquid distribution as indicated by the lower liquid distribution factor.

Figures 13 and 14 show the distribution of liquid conductivity over the whole cross-section of the column at the top plane (P6) and at P4 that was at 60 cm downward the column from P6. The axes labelled as direction are the two directions enclosing the cross-section of the column with the column center being at the center of the bar graph. As can be seen in these figures, liquid conductivity was more even at plane 4, indicating a better liquid distribution at this plane. When the tracer was introduced into the top of the column, it trickled down the column with the main liquid flow. There was some level of liquid mal-distribution at the top section of the packed bed. Therefore, the liquid distribution was less even, as indicated by a higher level of variation of the liquid conductivity at top plane (P6) with a standard deviation of 0.149 as compared with the value of 0.062 at P4. Moreover, this also indicates that the liquid conductivity measured by the ERT method could be used as an indicator for liquid distribution at various axial distances along the packed bed

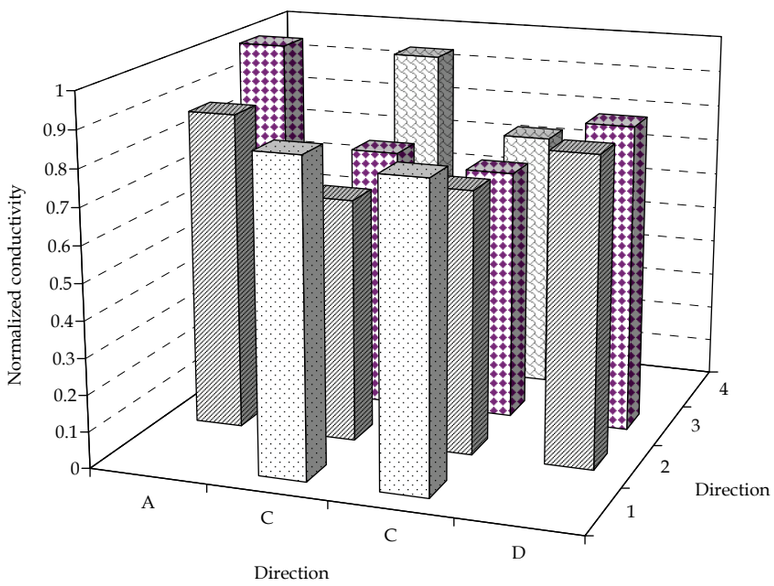

Fig. 13. Distribution of the conductivity across the column area at top plane (or P6)

4. Conclusion

In the present study, the ERT system was successfully applied to measure liquid flow distribution at varied axial distances along a packed bed without disturbing the flow profile.

In the upward flow mode, the liquid velocity and flow rate measured by the ERT system agreed to the velocity measured independently by a flow meter within 5%. A qualitative view of the images generated by the ERT system also provides information on the distribution within each plane. In addition, the ERT system could be used to capture radial and axial liquid maldistribution as well as liquid channelling in a trickle flow mode. For the trickle flow mode, the liquid residence time measured by the ERT method followed a similar trend of that calculated from the interstitial liquid velocity, which was determined from the liquid flowrate to the column and the packed bed characteristics. However, the calculated liquid residence time was about 1.5 – 2 times higher than that measured by the ERT method. This indicates the capability of the ERT method to capture the effect of liquid channelling, liquid hold-up and the wall flow on the actual liquid flow in a packed bed. The calculated superficial velocity is inaccurate since it is only true under an ideal condition with a perfect liquid distribution in the packed bed, which doesn't exist in reality.

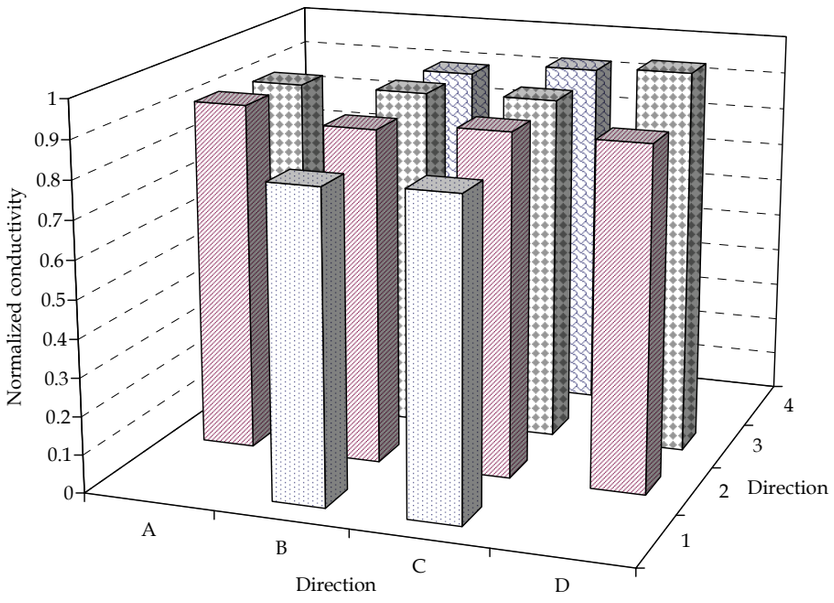

Fig. 14. Distribution of the conductivity across the column area at plane 4 (or P4 at 60 cm down the column from top plane)

5. Acknowledgement

Financial support from the National Science and Engineering Research Council of Canada (NSERC) for the purchase of the ERT system used in this project is highly appreciated. In addition, we would like to thank T. Vu and A. Nguyen for their assistance in the laboratory.

6. References

Aroonwilas, A.; Chakma, A.; Tontiwachwuthikul, P. & Veawab, A. (2003). Mathematical modeling of mass transfer and hydrodynamics in CO_2 absorbers packed with structured packings. *Chem. Eng. Sci.* Vol. 58, pp. 4037 – 4053.

Bolton, G. T.; Hooper, C.W.; Mann, R. & Stitt, E.H. (2004). Flow distribution and velocity measurement in a radial flow fixed bed reactor using electrical resistance tomography. *Chem. Eng. Sci.* Vol. 59, pp. 1989 – 1997.

Dang-Vu, T.; Doan, H.D. & Lohi, A. (2006a). Local mass transfer in a packed bed: Experiments and Model. *Ind. Eng. Chem. Res.* Vol. 45, pp. 1097-1104.

Dang-Vu, T.; Doan, H.D.; Lohi, A. & Zhu, Y. (2006b). A new liquid distribution factor and local mass transfer coefficient in a random packed bed. *Chem. Eng. J.* Vol.123, pp. 81 – 91.

Farid, M. M. & Gunn, D.J. (1978). Liquid distribution and redistribution in packed columns--II. Experimental. *Chem. Eng. Sci.* Vol. 33, pp. 1221 – 1231.

Gostick, J.; Doan, H.D.; Lohi, A. & Pritzker, M. (2002). Investigation of local mass transfer in a packed bed using a limiting current technique. *Ind. Eng. Chem. Res.* Vol. 42, pp. 3626 – 3634.

Guo, G. & Thompson, K.E. (2001). Experimental analysis of local mass transfer in packed beds. *Chem. Eng. Sci.* Vol. 56, pp. 121 – 132.

Hoek, P. J.; Wesselingh, A. & Zuiderweg, F.J. (1986). Small scale and large scale liquid maldistribution in packed columns. *Chem. Eng. Res. Des.* Vol. 64, pp. 431 – 449.

Inglezakis, V. J.; Lemonidou, M. & Grigoropoulou, H.P. (2001). Liquid holdup and flow dispersion in zeolite packed beds. *Chem. Eng. Sci.* Vol. 56, pp 5049 – 5057.

Kouri, R.J. & Sohlo, J. (1996). Liquid and gas flow patterns in random packings. *Chem. Eng. J.* Vol. 61, pp. 95 – 105.

Kumar, S.; Upadhyay, S.N. & Mathur, V.K. (1977). Low Reynolds number mass transfer in packed beds of cylindrical particles. *Ind. Eng. Chem. Process Des. Dev.* Vol. 16, pp. 1 – 8.

Kunjummen, B.; Prasad, T.S. & Sai, P.S.T. (2000). Radial liquid distribution in gas-liquid concurrent downflow through packed beds. *Bioproc. Eng.* Vol. 22, pp. 471 – 475.

Linek, V.; Moucha, T. & Rejl, F.J. (2001). Hydraulic and mass transfer characteristics of packings for absorption and distillation columns: Rauschert-Metal-Sattel-Rings. *Trans. IChemE* Vol. 79(A), pp. 725 – 732.

Loser, T.; Petritsch, G. & Mewes, D. (1999). Investigation of the two-phase countercurrent flow in structured packings using capacitance tomography, Proceedings of the 1st World Congress on Industrial Process Tomography, pp. 354– 361, Buxtion, Greater Manchester, April 14-17, 1999.

Macias-Salinas, R. & Fair, J.R. (1999). Axial mixing in modern packings, gas and liquid phases: I. single-phase flow. *AIChE J.* Vol. 45, pp. 222 – 239.

Reinecke, N. & Mewes, D. (1997). Investigation of the two-phase flow in trickle-bed reactors using capacitance tomography. *Chem. Eng. Sci.* Vol. 52, pp. 2111 – 2127.

Ruzinsky, F. & Bennington, C.P.J. (2007). Aspects of liquor flow in a model chip digester measured using electrical resistance tomography. *Chem. Eng. J.* Vol. 130, pp. 67 – 74.

Sedahmed, G. H.; El-Kayar, A.M.; Farag, H.A. & Noseir, S.A. (1996). Liquid solid mass transfer in packed beds of Raschig rings with upward two-phase (gas-liquid) flow. *Chem. Eng. J.* Vol. 62, pp. 61 – 65.

Tsochatzidis, N. A.; Karabelas, A.J.; Giakoumakis, D. & Huff, G.A. (2002). An investigation of liquid maldistribution in trickle beds. *Chem. Eng. Sci.* Vol. 57, pp. 3543 – 3555.

Yin, F.; Afacan, A.; Nandakumar; K. & Chuang, K.T. (2002). Liquid holdup distribution in packed columns: gamma ray tomography and CFD simulation. *Chem. Eng. Proc.* Vol. 41, pp. 473 – 483.

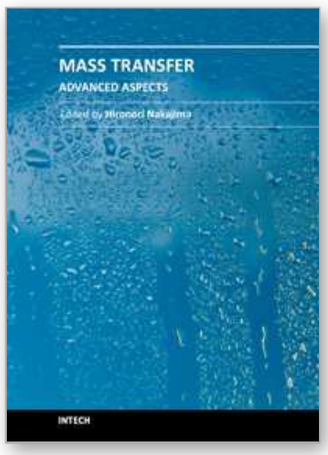

Mass Transfer - Advanced Aspects

Edited by Dr. Hironori Nakajima

ISBN 978-953-307-636-2
Hard cover, 824 pages
Publisher InTech
Published online 07, July, 2011
Published in print edition July, 2011

Our knowledge of mass transfer processes has been extended and applied to various fields of science and engineering including industrial and manufacturing processes in recent years. Since mass transfer is a primordial phenomenon, it plays a key role in the scientific researches and fields of mechanical, energy, environmental, materials, bio, and chemical engineering. In this book, energetic authors provide present advances in scientific findings and technologies, and develop new theoretical models concerning mass transfer. This book brings valuable references for researchers and engineers working in the variety of mass transfer sciences and related fields. Since the constitutive topics cover the advances in broad research areas, the topics will be mutually stimulus and informative to the researchers and engineers in different areas.

INTECH
open science | open minds

InTech Europe
University Campus STeP Ri
Slavka Krautzeka 83/A
51000 Rijeka, Croatia
Phone: +385 (51) 770 447
Fax: +385 (51) 686 166
www.intechopen.com

InTech China
Unit 405, Office Block, Hotel Equatorial Shanghai
No.65, Yan An Road (West), Shanghai, 200040, China
中国上海市延安西路65号上海国际贵都大饭店办公楼405单元
Phone: +86-21-62489820
Fax: +86-21-62489821

IntechOpen